IEEE Access
Multidisciplinary ⋮ Rapid Review ⋮ Open Access Journal

Received 7 January 2024, accepted 10 February 2024, date of publication 14 February 2024, date of current version 23 February 2024.

Digital Object Identifier 10.1109/ACCESS.2024.3366339

RESEARCH ARTICLE

Investigating Optimal Approaches for Energizations of DC Systems: The Stepwise Technique

GIOVANNI GARDAN[1], (Member, IEEE), AND GIAN CARLO MONTANARI[2], (Life Fellow, IEEE)
[1]Dipartimento di Ingegneria Industriale, Università degli Studi di Padova, 35131 Padua, Italy
[2]Center for Advanced Power Systems, Florida State University, Tallahassee, FL 32310, USA

Corresponding author: Gian Carlo Montanari (gmontanari@fsu.edu)

ABSTRACT The increasing presence of HVDC (High Voltage Direct Current) links and MVDC (Medium Voltage Direct Current) connections in transmission networks needs an in-depth knowledge of the mechanisms that could affect life and reliability of electrical asset components. As for all electrical systems in general, a crucial factor affecting availability of a HVDC asset is the insulation system reliability. One of the most common causes of premature electrical failure of asset components is electrical insulation breakdown or loss of serviceability. MV/HV extrinsic accelerated aging of organic insulation is mainly due to partial discharges (PD). Their presence, even if not promoting immediate breakdown, is almost a certain cause of apparatus life not matching specifications. This paper focuses on energizations on HVDC insulation systems, and, in general, supply voltage variations, which could be affected by PD due to manufacturing, laying, interface, or structural defects (as butt gaps). To minimize PD inception risk, a theory-driven, stepwise voltage application concept is proposed. The basic idea arises from the consideration that the factor playing a key role in PD inception is the jump voltage, and the electric field distribution in insulation during voltage transients is driven by permittivity (capacitance). Thus, energizing an insulation system with a first step lower than the partial discharge inception voltage in AC ($PDIV_{AC}$) and then growing voltage by smaller steps minimizing jump voltage would allow almost PD-free operation (apart from the risk of low-repetition PD at DC steady state if nominal voltage exceeds $PDIV_{DC}$). The effectiveness of this approach is proved by means of tests carried out on a simple test object consisting of flat XLPE (Crossed Linked Polyethylene) specimens with electrodes designed to cause surface PD, having available an innovative PD detection system which performs automatically and effectively both during voltage transients and in DC steady-state conditions. The experimental results show that the stepwise voltage energization, compared to the single step energization, could decrease significantly the number and magnitude of detected PD during energization transients, leading therefore the reduction of one order of magnitude of PD associated energy and relevant damage.

INDEX TERMS DC energization, high voltage energization, insulation systems, partial discharge modeling, partial discharge testing.

I. INTRODUCTION

HVDC (High Voltage Direct Current) transmission networks and MVDC (Medium Voltage Direct Current) distribution and industrial assets are rapidly growing being supported by continuous advancements in power electronics.

Unlike AC supply, however, there is much less on-field experience and knowledge of insulating material properties and aging processes under DC supply. Insulation system reliability, in short and long term, is a challenge that needs to be managed under different perspectives. One perspective is understanding long-term intrinsic aging mechanisms (those causing global aging under electrothermal stress), another is to model and infer the risk of extrinsic aging phenomena, particularly partial discharges (PD).

The associate editor coordinating the review of this manuscript and approving it for publication was Tariq Masood.

The type of electrical stress of DC insulation system is rather peculiar. In steady state, electric field is driven by conductivity, while during voltage transients (including energization and voltage polarity inversion), it is determined by permittivity, as in AC [1], [2]. Electric field transients, consequence, *e.g.*, of voltage steps, may last long times, from minutes to hours [2], [3]. Hence related phenomena (as field magnification along insulation thickness, [4], and partial discharges, [5], [6], [7], [8]) could affect insulation with accelerated intrinsic and extrinsic aging, possibly in non-negligible way, considering that a DC insulation system can be subjected to many thousands voltage transients during operation life [9].

Focusing on extrinsic aging due to partial discharges, the presence of defects in the bulk, at interfaces or on the surface of insulation systems can trigger partial discharges during voltage transients, which might not be present in DC steady state. It has been shown in [10] that the partial discharge inception voltage in AC, $PDIV_{AC}$, can be significantly lower than that in DC ($PDIV_{DC}$), especially at low-load insulation temperatures. Hence, PD may incept when a voltage step is applied to energize an insulation (or provide polarity inversion), even if the nominal DC voltage is lower than $PDIV_{DC}$, when the field magnitude exceeds that for AC PD inception. This can hold for both internal and surface discharges. Estimates of partial discharge inception field, *PDIE*, and voltage, can be achieved through the three-leg approach described in section III, for internal and surface discharges, and both AC and DC [11], [12].

The rationale behind the idea described and validated in this paper is that to reduce the risk of PD inception during DC energization (or voltage polarity inversion), a stepwise voltage waveform can be applied instead of a single voltage step. Nowadays the single step voltage energization is the conventional way to energize MVDC/HVDC systems, but such procedure could increment the risk of PD inception due to high jump voltage. Thus, to overcome this limitation, we propose here the stepwise voltage waveform energization (characterized by the succession of smaller jump voltages), which could be a valid alternative reducing PD inception risk and PD intensity caused by energizations.

The fundamental assumption, to be proved here, is that if the magnitude of each voltage step, also called jump voltage (concept defined in [13]), is lower than the corresponding $PDIV_{AC}$ of the test object, the energizations can be PD-free or, at least, it could be characterized by a much lower amount of PD pulses and smaller PD magnitude. The whole operation of the insulation system can, therefore, minimize PD occurrence if also $PDIV_{DC}$ is lower than the nominal, steady state, voltage.

II. EXPERIMENTAL SET-UP AND MATERIALS

The experimental set-up was designed to trigger surface PD by a simple test object, which should be able to establish the validity of the proposed idea. To this purpose, a Crossed Linked Polyethylene (XLPE) single-layer dielectric specimen (press-molded, mean thickness of 0.8 mm) was used, with electrodes designed properly (see Fig. 1) for the purpose of incepting discharges along specimen surface, as previously demonstrated in [11] and [12]. Such electrodes are made of brass and were placed at different distances on XLPE specimen surface, but most of the following results refer to a distance of 10 mm, see Fig. 1. Both the power supply circuit and signal circuit are sketched in Fig. 2. A DC power supply remotely controlled by a PC was used to energize the HV electrode. PD pulses were detected though a High Frequency Current Transformer (HFCT, bandwidth: 100 kHz-50 MHz) placed on the ground return of the power circuit. The HFCT was connected to a partial discharge analyzer (PDA), which was connected to a PC equipped with an innovative acquisition and analytics software (based on Separation, Recognition and Identification, SRI) for PD monitoring and acquisition (see [15]).

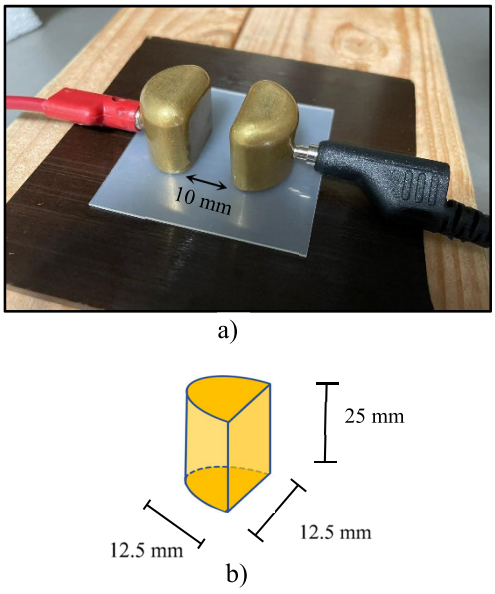

FIGURE 1. (a) Electrode configuration used to trigger surface PD on a XLPE single layer material under test, (b) The main geometric dimensions of the electrodes used for the experimental activity.

All experiments were conducted at atmospheric pressure and temperature (20 °C).

III. PDIV ESTIMATION AND THE THREE-LEG APPROACH

As mentioned, $PDIV_{AC}$ is the parameter to be considered when applying stepwise voltage energizations to the test object, in order to reduce PD occurrence during voltage transients. A recent new framework for PD-free design of insulation systems, the so called "three leg-approach" [14], could be exploited for the estimation of $PDIV_{AC}$ for surface discharges.

This approach is valid for both AC and DC systems, and it is based on three steps (the "legs"), which are:

1) Electric field simulation of the object under study (first leg);

2) Modelling of the PD inception field and voltage for the object under study (second leg);
3) PD measurements to validate the results predicted by legs 1, 2 (third leg);

Specifically, the voltage at which the maximum (approximately) electric field in an insulation system (calculated at leg 1) matches the PD inception field estimated by the model at leg 2 is the partial discharge inception voltage.

Eventually, experimental validation is performed (leg 3) in order to support *PDIV* estimation thus obtained. *PDIV* measurements must be carried out with the support of hardware/software tools allowing recognition and identification of the different typologies of source generating PD, *i.e.* internal, surface and corona discharge (according to descending order of harmfulness) [15], [16], [17].

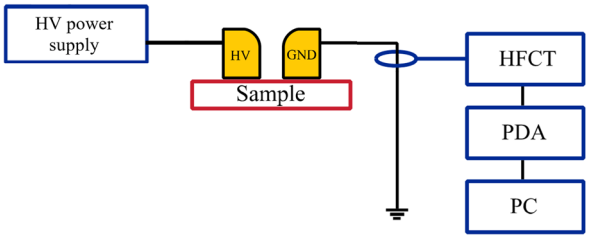

FIGURE 2. Sketch of the test set-up used for the experiments.

A. FIRST LEG: ELECTRIC FIELD SIMULATION

In the specific test arrangement considered in this work, Figs. 1, 2, simulations by means of the FEM (Finite Element Method) software COMSOL Multiphysics©were carried out to compute the tangential (surface) electric field (first leg). Figure 3 represents the implemented geometry of the XLPE layer specimen, with HV (high voltage) and GND (ground) electrodes, whereas Fig. 4 depicts a zoom of the tangential field under the application of 1 kV of voltage, from the triple point O to 1 mm of distance. Electrode contour was modelled considering a curvature radius, ρ, of 100 μm.

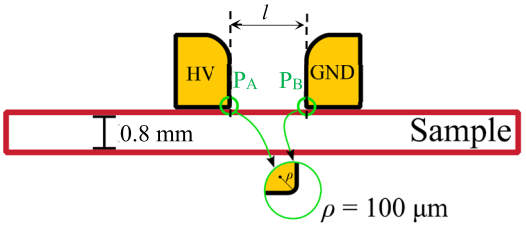

FIGURE 3. Geometric model implemented to calculate the tangential and orthogonal electric field profiles on the XLPE sample surface. HV and GND represent the HV supply and the ground-connected electrodes, respectively.

B. SECOND LEG: PD INCEPTION MODELLING

The generalized model for PD inception (second leg) is given by [11], [12], [18]:

$$E_{inc} = \left(\frac{E}{p}\right)_{cr} p\left[1 + \frac{B}{(plk_s)^{\beta}}\right] \tag{1}$$

where $(E/p)_{cr}$ is the critical reduced field at atmospheric pressure, p is pressure, l is the distance on the surface from the HV and GND (P_A and P_B in Fig. 3), B and β are empirical parameters, k_s is a scale parameter which takes into account the extent of field divergence at triple point, being $=1$ for uniform field distribution and $\ll 1$ for large field gradients [11], [12]. The parameter values of (1) are reported in Tab. 1 for the test object of Figs. 1 and 3.

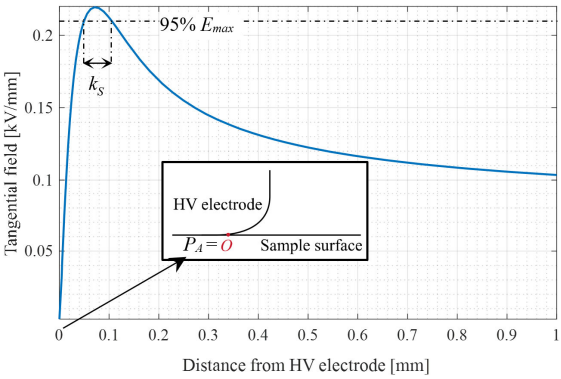

FIGURE 4. Tangential electric field profile (from the HV electrode to ground at 1mm from HV) under the application of 1kV to the test object of Fig. 3. The reference "O" represents the triple point (P_A of Fig. 3).

The value of surface $PDIV_{AC}$ can be obtained by simulation, varying the applied voltage until the maximum field in Fig. 4 intersect the value provided by (4), or, more simply, by exploiting the linearity of the Laplace equation:

$$\frac{PDIV_{AC}}{V_{sim}} = \frac{E_{inc}}{E_{p,sim}}. \tag{2}$$

where V_{sim} is the applied voltage in the simulation, E_{inc} is the surface inception field computed by (1), and $E_{p,sim}$ is the peak of the surface field considering the applied voltage V_{sim}.

The surface $PDIV_{AC}$ thus calculated is 7.2 kV. This would mean that DC steps lower than $7.2{\cdot}\sqrt{2}$ =10.2 kV (since the $PDIV_{AC}$ value refers to the Root Mean Square, RMS, value) should allow PD-free energization. This is proved in the Sect. IV-A.

C. THIRD LEG: PDIV MEASUREMENTS

$PDIV_{AC}$ and $PDIV_{DC}$ parameters of the test set-up of Fig. 1 and 3 were determined according to the method validated in [11] and [12]. For $PDIV_{AC}$, measurements were conducted by increasing stepwise AC voltage and acquiring PD for 10 seconds, at each voltage level. This procedure had to be repeated till the measured $PDIV_{AC}$ values was reached, *i.e.*, the voltage level at which PD activity starts persistently (IEC 60270, [19]). After taking several measurements for the same test arrangement, the mean value of the measurements was taken as the best estimate, and its uncertainty was computed according to a type A evaluation [20]. To take repeated measurements after the de-energization of the XLPE specimen, enough time was waited to be sure that residual space charge due to previous PD was depleted (a thermal

treatment was also adopted). The combination of such waiting time (1 hour) and thermal treatment (heating of the specimen up to 80 °C) has been shown to be effective in depleting residual space charges.

Likewise, $PDIV_{DC}$ measurements were carried out by increasing stepwise DC voltage, but with steps lasting at least 5 min, and acquiring PD during voltage increase transients and in steady state. The reason of these higher time steps, with respect to the $PDIV_{AC}$ measurement, is twofold: achieving a robust estimation of $PDIV_{DC}$ (indeed, repetition rate in DC is much smaller than in AC), and approaching DC steady-state electric condition considering that most of PD occur within a fraction of the time constant (*e.g.,* 10%) [6].

TABLE 1. Parameter estimates of model (1) applied to surface discharges, *ks* value for the field profile of Fig. 4 and surface PD inception field obtained by model (1).

Quantity	$(E/p)_{cr}$	B	β	ks	E_{inc}
Unit	V $Pa^{-1}m^{-1}$	$Pa^{1/2}m^{1/2}$	-	mm	kV/mm
Value	8.0	4.3	2	0.06	2.2

TABLE 2. Surface $PDIV_{AC}$ and $PDIV_{DC}$ measurement values, mean values and 98% confidence intervals.

Acquisition	$PDIV_{DC}$ Measurements [kV]	$PDIV_{AC}$ Measurements [kV]
1st	10.5	8.2
2nd	10.9	7.3
3rd	10.6	8.7
4th	10.1	7.8
5th	10.2	8
$PDIV_{DC}$= 10.5 ± 1.2 kV $PDIV_{AC}$= 8.0 ± 1.9 kV		

Table 2 summarizes the results of surface $PDIV_{AC}$ and $PDIV_{DC}$ measurements for the test arrangement of Figs. 1, 3.

Considering $PDIV_{AC}$, the estimation by the first two legs (*i.e.* 7.2 kV) is close to the measurement (*i.e.* 8 ± 1.9 kV/mm), since it lies within the 98% confidence interval (computed according to the standard Type A evaluation of uncertainty [20]).

Similarly, considering the $PDIV_{DC}$, the estimated value is equal to 9.5 kV and lies within the 98% confidence interval of the measurement (*i.e.* 10.5 ± 1.2 kV/mm).

As regards the estimation of the $PDIV_{DC}$ value, it is worth reminding the importance of having accurate conductivity values of the tested insulating material, since the accuracy of the simulated field, and, thus, of the PD inception field, depends on them (electric field in DC is driven by conductivity, at least in steady state [1]). Bulk and surface conductivities are a function of temperature and electric field. An approximate expression is given by [12]:

$$\sigma\,(T, E) = \sigma_0 \exp\left[\alpha(T - T_0) + \beta(E - E_0)\right], \qquad (3)$$

where T_0 and E_0 are reference temperature and field, T and E are actual temperature and applied field, α and β are temperature and field coefficients, and σ_0 is the reference conductivity of the tested material at $T{=}T_0$ and $E{=}E_0$. Based on experiments, the values of σ_0 for the XLPE specimens used for this research work were taken $= 2.8{\cdot}10^{-17}$ S/m for bulk conductivity, and $= 5{\cdot}10^{-15}$ S/m, for surface conductivity. A thorough knowledge of the air conductivity σ_{air} is also fundamental to compute the DC surface field profile. A reasonable value of σ_{air} near the earth surface is 10^{-14} S/m [12], [21], and this value was considered in the simulations.

IV. EXPERIMENTAL OBSERVATIONS FROM DIFFERENT ENERGIZATION TECHNIQUES

A. PD OCCURRENCE DURING ENERGIZATION WITH DIFFERENT STEP MAGNITUDE

Generally, PD incept during voltage rise or fall, *i.e.*, during positive of negative variations of the voltage waveform over the time (dv/dt). Since during voltage transients the electric field distribution in insulation is driven by permittivity, as in AC, an energization with a jump voltage lower than the $PDIV_{AC}$ should be, from a theoretical standpoint, free of PD. The purpose of this sub-section is to experimentally validate the above-mentioned assumption.

TABLE 3. Experimental results of PD measurements after the application of voltage steps of various amplitude.

Step applied	PD during transients?	N. of PD	>$PDIV_{AC}$?
Step 0-5 kV	No	0	<$PDIV_{AC}$
Step 0-6 kV	No	0	<$PDIV_{AC}$
Step 0-7 kV	Yes	1	<$PDIV_{AC}$
Step 0-8 kV	Yes	2	<$PDIV_{AC}$
Step 0-9 kV	Yes	3	<$PDIV_{AC}$
Step 0-10 kV	Yes	4	<$PDIV_{AC}$
Step 0-11 kV	Yes	4	<$PDIV_{AC}$
Step 0-12 kV	Yes	21	>$PDIV_{AC}$
Step 0-13 kV	Yes	75	>$PDIV_{AC}$
Step 0-15.8 kV	Yes	89	>$PDIV_{AC}$

Table 3 reports the experimental results with the application of voltage steps of different amplitude, in order to confirm that during fast voltage transients there is inception of PD only for magnitude larger than that corresponding to the $PDIV_{AC}$ of object under test. Since the measured mean value of $PDIV_{AC}$ is equal to 8.0 kV, the experimental results confirm that persistent PD activity is incepted only for steps of voltage whose magnitude is:

$$V_{step} > 8\sqrt{2} = 11.3\text{kV}.$$

Indeed, very few PD pulses are recorded at voltage steps lower than 11 kV.

B. ENERGIZATION BY A SINGLE STEP VOLTAGE: EXPERIMENTAL OBSERVATIONS

To carry out an experimental comparison of the stepwise with voltage energization (described in Sect. IV-C) with the conventional single-step procedure, first a single step of 15.8 kV = 1.5 $PDIV_{DC} \simeq 2$ $PDIV_{AC}$, slew rate = 1000 kV/min, was applied to the XLPE specimen in order to observe PD activity due to a fast voltage transient. The recorded PD activity, by means of the SRI software, is reported in Fig. 5. It is worth noting that PD magnitude slightly decreases towards the steady state DC voltage. As regards repetition rate 89 pulses were recorded in the first 35 seconds, but most of those occur in the first 10 s, which is the time interval in which most of the field transient occurs.

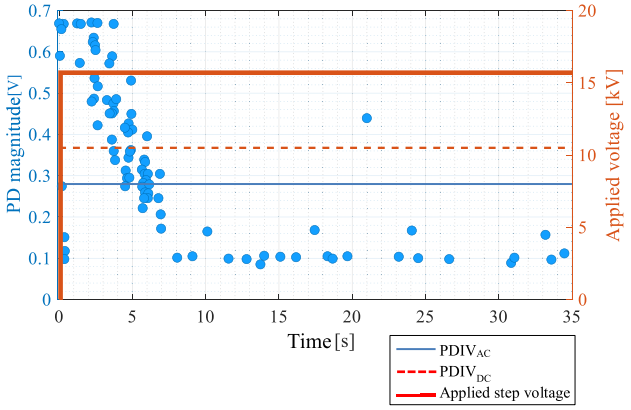

FIGURE 5. PD activity after the application of a single voltage step (at t=0s) corresponding to 1.5$PDIV_{DC}$.

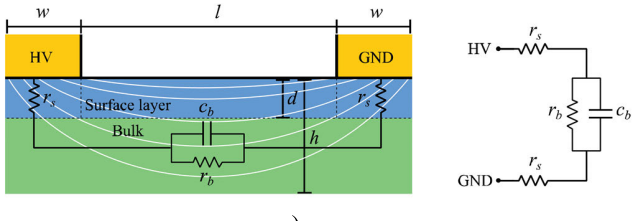

a)

Physical parameters	Geometrical parameters	Equivalent circuit parameters
$\varepsilon_0 = 8.85 \cdot 10^{-12}\,C^2N^{-1}m^{-2}$ $\varepsilon_{rb} = 2.3$ $\sigma_s = 5 \cdot 10^{-15}\,Sm^{-1}$ $\sigma_b = 2.8 \cdot 10^{-17}\,Sm^{-1}$	$d = 100\mu m$ $h = 0.8mm$ $l = 10mm$ $w = 12.5mm$	$r_s = 1.6 \cdot 10^{12}\,\Omega \cdot m$ $r_b = 5.1 \cdot 10^{17}\,\Omega \cdot m$ $c_b = 1.4 \cdot 10^{-12}\,F \cdot m$
$\tau = \frac{2r_s r_b}{r_s + r_b} \cdot c_b = 4.6\ s$		

b)

FIGURE 6. (a) Equivalent circuit used for the estimation of the time constant describing the evolution of the electric field transient. This equivalent circuit is developed by following the electric field lines going from the high voltage electrode to the ground one and passing through the dielectric specimen. (b) Physical and geometrical data, equivalent circuit parameters, and time constant computation for the specific test arrangement under study (Fig. 1), from [3].

The time constant, τ, of the electric field transient after the application of a DC step voltage, in fact, is given by [3]:

$$\tau = \frac{2r_s r_b}{r_s + r_b} \cdot c_b, \tag{4}$$

where r_s, r_b, c_b are the parameters of the equivalent circuit drawn in Fig. 6 which describes the test arrangement of Fig. 1. These circuit parameters depend on the geometry (*i.e.* electrode widths w, surface layer thickness d, sample thickness h, and distance between electrodes l) and material characteristics (*i.e.* absolute permittivity $\varepsilon_0\varepsilon_{rb}$, surface conductivity σ_s, and bulk conductivity σ_b, see Fig. 6). The time constant estimated from (3) is 11.4 s, meaning that the electric field reaches the steady-state condition completely about after 50s, but most of the transient occurs in the first 10s. This fits to the results of Fig. 5, which clearly show a drastically decreased PD activity (both for repetition rate and magnitude) after τ, with some remaining low repetition rate, PD pulses for t> τ, which can be a mix up of residual transient and of steady state DC PD events (the test voltage is larger also than $PDIV_{DC}$).

This indicates that if the $PDIV_{AC}$ is exceeded, PD repetition rate can be significant at each energization or voltage polarity inversion. This would be sufficient to cause damage to insulation, which, with repeated transients, would translate into thus accelerated aging and premature failure.

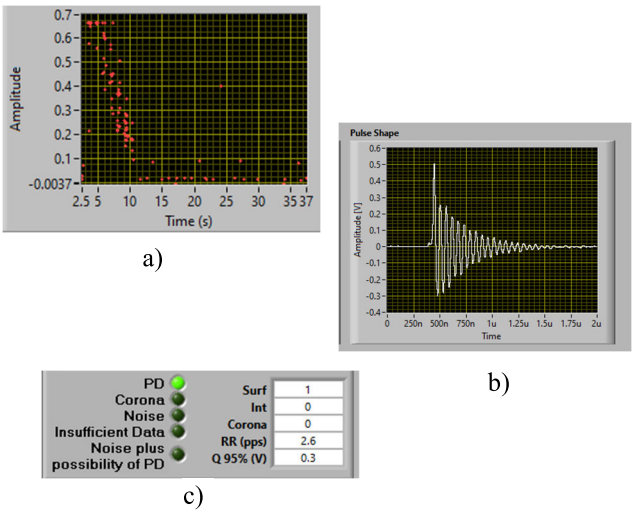

a) b) c)

FIGURE 7. Time-resolved PD (TRPD) pattern after test cell energization by means of a single-step corresponding to 1.5$PDIV_{DC}$ (a), example of PD pulse acquired during the transients (b), identification of the typology of PD (c).

Figure 7 shows the graphical interface of the SRI innovative automatic acquisition and analytics software used for these measurements, based on separation, recognition and identification (SRI), as described in [15], [16], and [17].

Specifically, Fig. 7a depicts the time-resolved pattern taken from a screenshot of the innovative, automatic software used for PD experiments, and Fig. 7b represents an example of partial discharge pulse extracted from the PD acquisition

during the transient. Eventually, Fig. 7c reports the identification of the typology of defect generating PD (surface with likelihood 1), which confirms that the test cell of Figs. 1 and 3 triggers surface PD. It is noteworthy that since identification is based on a fuzzy logic engine, likelihood could be a number between 1 (certainty) and 0.

C. STEPWISE ENERGIZATION: EXPERIMENTAL OBSERVATIONS

In order to prove the effectiveness, in terms of impact on PD magnitude and repetition rate, of the stepwise energization approach with voltage steps$<PDIV_{AC}$, experimental observations by using the material and test set-up described above and represented in Fig. 1, 2, 3 were carried out.

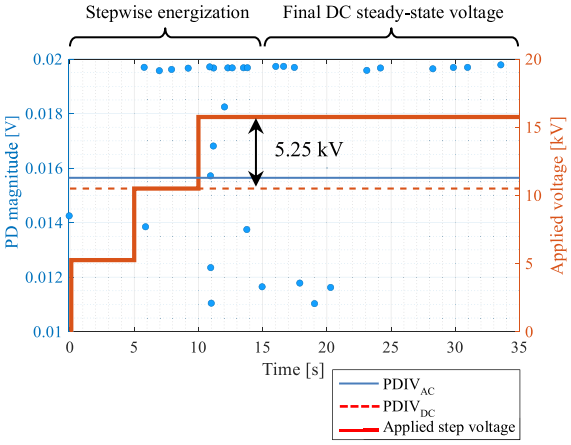

FIGURE 8. PD activity recorded by means of the SRI software after the application of stepwise energization till the DC steady-state value of 1.5PDIV$_{DC}$. Each voltage step (<PDIV$_{AC}$) lasts 5 seconds. The different impact, in terms of PD, with the case of single-step energization (see Fig. 5) is dramatic: it is evident the lower number of PD pulses (i.e., lower repetition rate) and the lower charge magnitudes, meaning that the insulation system is subjected to a minor degradation.

Voltage was applied by the procedure sketched in Fig. 8, consisting of the application of three steps of 5.25 kV each (thus lower than 50% $PDIV_{AC}$, *i.e.,* $8\sqrt{2} = 11.3$kV), duration of 5 s (during which good part of the electric field transient has occurred) up to 1.5 $PDIV_{DC}$ (*i.e.,* 15.8 kV). PD monitoring was carried out during the application of the whole energization procedure (see blue dots in Fig. 8).

Table 4 highlights a comparison between the single and the multiple step procedures, providing PD mean repetition rate, mean charge magnitude and a quantity which can be related to insulation degradation, that is, the transient energization damage rate due to partial discharges, D_r [22], [23], *i.e.,*

$$D_r = F_D(\Sigma_i q_i) \tag{5}$$

where q_i (in V) is charge magnitude at time t_i, and F_D a damage factor depending on the fraction of effective hot electrons contributing to damage, which can be taken = 0.02, according to [23]. Index i refers to the i^{th} event occurring during energization time Δt. The value of Δt=15 s, based on Figs. 5, 8 and the time constant value, is taken for Table 4.

TABLE 4. Comparison between single step and stepwise energizations as regards mean repetition rate (rr_m), mean charge magnitude (q_m) and energization damage density (D_d) eq. (4), with reference to Figs. 5, 9 and Δt=15 s.

	Single Step Energization	Stepwise Energization
Mean PD repetition rate rr_m [1/s]	4.9	1.3
Mean PD charge magnitude q_m [V]	0.381	0.017
PD Damage density D_d	0.564	0.007

Figure 8 and Table 4 highlight that, on the whole, the total number of observed PD is nearly four times lower with respect to the single step energization (see Fig. 5), and the mean PD charge amplitude is roughly 22 times lower. The decrease of these two parameters due to the stepwise energization brings the PD associated energy 81 times lower with respect to the single step energization, meaning that the stepwise energization procedure reduces the global PD damage of 99% for the object under assessment (see damage density values of Tab. 4), according to the damage density definition (4). This proves the idea behind this alternative energization procedure.

It is noteworthy that the test procedure studied here reaches a final voltage value which is larger than $PDIV_{DC}$, see Table 2, in order to enable detection of both transient and steady-state PD. It can be seen, indeed, that while there are not PD till $PDIV_{DC}$ (thus confirming that rising voltage by steps lower than $PDIV_{AC}$ does not incept PD), after the application of the second step (see Fig. 8), an increasing PD activity, at very low repetition rate (as expected under DC voltage) is detected, since this step brings to a voltage slightly higher than $PDIV_{DC}$ and very near to $PDIV_{AC}$.

Summarizing, it can be speculated that an optimized procedure which would minimize the energization (or voltage polarity inversion) time, could consist of applying first a step slightly lower than $PDIV_{AC}$, e.g., 0.9 $PDIV_{AC}$, then go by fine tuning to the nominal voltage, V_N, applying a number of steps of, e.g., 0.2 V_N, all $< PDIV_{AC}$.

V. CONCLUSION

A stepwise voltage application strategy to be adopted during energization of any DC electrical apparatus is proposed and validated successfully. The idea stems from the rationale that the jump voltage occurring during step-energizations might trigger PD and related extrinsic aging for an insulation system if it exceeds the $PDIV_{AC}$. The small amount of PD-related extra aging caused by an energization or voltage polarity inversion may translate into premature failure, to an extent that depends on the voltage transient rate during insulation system operation life.

Validation relies upon the three-leg approach (methodology which gathers coherently field computation, inception modelling, and PD measurements), and experimental observations are conducted by the support of an innovative

hardware and software solution (SRI software) allowing automatic monitoring of PD activity and identification of PD source typology, both during transients and in DC steady state.

The comparison between two different energization procedures, that is, single-step and the proposed stepwise energization, shows that the latter brings to one quarter of the number of PD pulses, 99% reduction of PD damage and large decrease of PD magnitude.

The concept presented in this work could open a path towards the development of strategies to be adopted whenever sudden voltage changes (energizations, voltage inversion, and step-variation voltage) are required in the MV and HV DC electrical equipment.

REFERENCES

[1] C. K. Eoll, "Theory of stress distribution in insulation of high-voltage DC cables part II," *IEEE Trans. Electr. Insul.*, vol. EI-10, no. 2, pp. 49–54, Jun. 1975.

[2] G. Mazzanti and M. Marzinotto, *Extruded Cables for High Voltage Direct Current Transmission: Advance in Research and Development*. Hoboken, NJ, USA: Wiley, Jul. 2013.

[3] H. Naderiallaf, P. Seri, and G. C. Montanari, "On the calculation of the dielectric time constant of DC insulators containing cavities," in *Proc. IEEE Conf. Electr. Insul. Dielectric Phenomena (CEIDP)*, Vancouver, BC, Canada, Dec. 2021, pp. 623–626.

[4] P. Cambareri, C. de Falco, L. D. Rienzo, P. Seri, and G. C. Montanari, "Electric field calculation during voltage transients in HVDC cables: Contribution of polarization processes," *IEEE Trans. Power Del.*, vol. 37, no. 6, pp. 5425–5432, Dec. 2022.

[5] P. H. F. Morshuis and J. J. Smit, "Partial discharges at DC voltage: Their mechanism, detection and analysis," *IEEE Trans. Dielectr. Electr. Insul.*, vol. 12, no. 2, pp. 328–340, Apr. 2005.

[6] H. Naderiallaf, P. Seri, and G. C. Montanari, "Effect of voltage slew rate on partial discharge phenomenology during voltage transient in HVDC insulation: The case of polymeric cables," *IEEE Trans. Dielectr. Electr. Insul.*, vol. 29, no. 1, pp. 215–222, Feb. 2022.

[7] H. Naderiallaf, P. Seri, and G. C. Montanari, "Designing a HVDC insulation system to endure electrical and thermal stresses under operation. Part I: Partial discharge magnitude and repetition rate during transients and in DC steady state," *IEEE Access*, vol. 9, pp. 35730–35739, 2021.

[8] H. Naderiallaf, P. Seri, and G. C. Montanari, "Investigating conditions for an unexpected additional source of partial discharges in DC cables: Load power variations," *IEEE Trans. Power Del.*, vol. 36, no. 5, pp. 3082–3090, Oct. 2021.

[9] J. C. Das, *Transients in Electrical Systems: Analysis, Recognition, and Mitigation*. New York, NY, USA: McGraw-Hill, 2010.

[10] H. Naderiallaf, R. Ghosh, P. Seri, and G. C. Montanari, "HVDC insulation systems: Effect of voltage polarity inversion slew rate on partial discharge phenomenology and harmfulness," in *Proc. 22nd Int. Symp. High Voltage Eng.*, Xi'an, China, Nov. 2021, pp. 7–12.

[11] P. Cambareri and G. Montanari, "A surface discharge model for the design of surface components of insulation systems under AC stress in industrial electronics environments," *IEEE J. Emerg. Sel. Topics Ind. Electron.*, vol. 4, no. 2, pp. 698–706, Apr. 2023.

[12] P. Cambareri and G. Montanari, "A surface discharge model for partial discharges under DC stress," *IEEE J. Emerg. Sel. Topics Ind. Electron.*, early access, Aug. 1, 2024, doi: 10.1109/JESTIE.2023.3299836.

[13] *Rotating Electrical Machines—Part 18–41: Partial Discharge Free Electrical Insulation Systems (Type I) Used in Rotating Electrical Machines Fed From Voltage Converters—Qualification and Quality Control Tests*, IEC Standard 60034-18-41, 2014.

[14] G. C. Montanari, D. Nath, and P. Cambareri, "A new approach to the design of surface subsystems of polymeric insulators for HV and MV apparatus under AC voltage," *High Voltage*, vol. 8, no. 4, pp. 651–658, Jun. 2023.

[15] G. C. Montanari and R. Ghosh, "An innovative approach to partial discharge measurement and analysis in DC insulation systems during voltage transient and in steady state," *High Voltage*, vol. 6, no. 4, pp. 565–575, Aug. 2021.

[16] R. Ghosh, P. Seri, and G. C. Montanari, "A track towards unsupervised partial discharge inference in electrical insulation systems," in *Proc. IEEE Electr. Insul. Conf. (EIC)*, Jun. 2020, pp. 190–193.

[17] G. C. Montanari, S. Schwartz, Q. Yang, D. Nath, R. Ghosh, and R. Cuzner, "Towards partial discharge automatic and unsupervised monitoring: A technological breakthrough for MV electrical asset condition monitoring and diagnostics," in *Proc. 9th Int. Conf. Condition Monitor. Diagnosis (CMD)*, Kytakyushe, Japan, Nov. 2022, pp. 588–592.

[18] L. Niemeyer, "A generalized approach to partial discharge modeling," *IEEE Trans. Dielectr. Electr. Insul.*, vol. 2, no. 4, pp. 510–528, Aug. 1995.

[19] *High-Voltage Test Techniques—Partial Discharge Measurements*, IEC Standard 60270, 3.1 Edition, Nov. 2015.

[20] *Guide To the Expression of Uncertainty in Measurement. GUM 1995 with Minor Corrections*, document GUM-100, BIPM, IEC, IFCC, ILAC, ISO, IUPAC, IUPAP, OIML, 2008.

[21] E. Seran, M. Godefroy, E. Pili, N. Michielsen, and S. Bondiguel, "What we can learn from measurements of air electric conductivity in ^{222}Rn-rich atmosphere," *Earth Space Sci.*, vol. 4, no. 2, pp. 91–106, Feb. 2017.

[22] S. Serra, G. C. Montanari, and G. Mazzanti, "Theory of inception mechanism and growth of defect-induced damage in polyethylene cable insulation," *J. Appl. Phys.*, vol. 98, no. 3, pp. 1–15, Aug. 2005.

[23] L. Sanche, "Nanoscopic aspects of electronic aging in dielectrics," *IEEE Trans. Dielectr. Electr. Insul.*, vol. 4, no. 5, pp. 507–543, Oct. 1997.

GIOVANNI GARDAN (Member, IEEE) was born in Venice, Italy, in 1995. He received the B.S. degree in energy engineering and the Dr.-Ing. degree in electrical engineering from Università degli Studi di Padova, in 2017 and 2020, respectively, where he is currently pursuing the Ph.D. degree in industrial engineering. His main fields of research are power systems modeling and high-voltage electrical engineering. He is a Young Member of Cigrè and AEIT.

GIAN CARLO MONTANARI (Life Fellow, IEEE) is currently a Research Faculty III with the Center for Advanced Power Systems (CAPS), Florida State University, USA; an Alma Mater Professor with the University of Bologna, Italy; and an Adjunct Professor with Institut Teknologi Bandung, Indonesia. He has been a Full Professor of electrical technology with the Department of Electrical, Electronic and Information Engineering, University of Bologna, teaching courses on electrical technology, reliability, and asset management. Since 1979, he has been working in the field of aging and endurance of insulating materials and systems, diagnostics of electrical systems, asset management, and innovative electrical materials (magnetics, electrets, super-conductors, and nano-materials). He has engaged in the fields of power quality and energy market, power electronics, reliability and statistics of electrical systems, and smart grids. He was the Founder and the President of spin-off Techimp, established in 1999. He is the author or coauthor of more than 800 scientific articles. He has been recognized with several awards, including the IEEE Ziu-Yeda, the Thomas W. Dakin Award, the Whitehead Prize, the Eric Forster Award, and the IEC 1906 Awards.

Open Access funding provided by 'Università degli Studi di Padova' within the CRUI CARE Agreement